Int. J. Heat Mass Transfer. Vol. 35, No. 11, pp. 3095–3104, 1992
Printed in Great Britain

0017–9310/92 $5.00 + 0.00

A two-equation heat transfer model for predicting turbulent thermal fields under arbitrary wall thermal conditions

M. S. YOUSSEF, Y. NAGANO and M. TAGAWA
Department of Mechanical Engineering, Nagoya Institute of Technology, Gokiso-cho, Showa-ku, Nagoya 466, Japan

(*Received* 31 *July* 1991 *and in final form* 19 *November* 1991)

Abstract—A new proposal for the $\overline{t^2}$–ε_t heat transfer model is presented along with an accurate prediction of wall turbulent thermal fields. The proposed model reproduces the correct wall limiting behavior of velocity and temperature under arbitrary wall thermal conditions. Assessment of the model constants and functions are made to generalize applicability of the $\overline{t^2}$–ε_t model. The proposed model is tested with five different typical thermal fields, which often occur in engineering applications, in wall turbulent shear flows. The predicted results are compared with the available experimental and full simulation data, together with the previous model predictions. It is shown that the present model works much better than the previous models.

1. INTRODUCTION

THE TURBULENCE model for heat transfer is a set of differential equations which, when solved with the mean-flow and turbulence Reynolds stresses equations, allow calculations of relevant correlations and parameters that simulate the behavior of thermal turbulent flows. Like the classification of turbulence models for the Reynolds stresses, the phenomenological turbulent heat transfer models are classified into zero-equation, two-equation, and heat-flux equation models.

The zero-equation heat transfer model is a typical and most conventional method for analyzing the turbulent heat transfer, in which the eddy diffusivity for heat α_t is prescribed via the known eddy viscosity ν_t together with the most probable turbulent Prandtl number Pr_t, so that $\alpha_t = \nu_t/Pr_t$. Many previous studies have, however, revealed that there are no universal values of Pr_t even in simple flows [1] (e.g. at the same streamwise location, a value of Pr_t close to the wall is different from that away from the wall [2, 3]), and this lack of universality restricts the applicability of a zero-equation model. On the other hand, a heat-flux equation model ought to be more universal, at least in principle. This model, however, is still rather primitive and the results are not as satisfactory as initially expected, mainly owing to a few unreasonable hypotheses in the model. (With regard to some detailed problems and recent progress, see, for example, Nagano and Tagawa [4–6].)

For a velocity field, the k–ε model of turbulence is now regarded as a powerful tool for predictions of many complex flow problems including jets, wakes, wall flows, reacting flows, and flows with centrifugal and Coriolis forces [7]. As for scalar turbulence, Nagano and Kim [8] developed a two-equation model for heat transport (hereinafter referred to as the NK model). They modeled the eddy diffusivity for heat α_t using the temperature variance $\overline{t^2}$ and the dissipation rate of temperature fluctuations ε_t, together with k and ε. The NK model is applicable to thermal fields where a real value Pr_t is unknown, and thus has universality much higher than the conventional zero-equation model. It correctly predicts the thermal fields in boundary layers, channel flows and free shear flows [8, 9], though a slight change in model constants is needed in the last case as in the k–ε model [10, 11]. A weakness is that the NK model has been developed aiming mainly at the heat transfer analysis under the uniform wall-temperature condition. Consequently, in order to analyze heat transfer problems under various wall thermal conditions, we need further improvements of the NK model or development of a more sophisticated $\overline{t^2}$–ε_t heat transfer model.

In the present study, we develop a new $\overline{t^2}$–ε_t model, maintaining the original conception of the NK model. Using the Taylor series expansion for the energy equation in the near-wall region, we make it clear how the wall limiting behavior of turbulence quantities in a thermal field varies with a wall thermal condition, and then we construct the basic modeled equations to satisfy these requirements. As a turbulence model for a velocity field, we use a low-Reynolds-number type k–ε model of Nagano and Tagawa [12], which is developed to make the model of Nagano and Hishida [13] satisfy the physical requirements of the limiting behavior of wall and free turbulence.

The present heat transfer turbulence model was tested by application to turbulent boundary layers with five different wall thermal fields; namely, a uniform wall temperature, a uniform wall heat flux, a

NOMENCLATURE

A_μ, B_μ turbulence model constants for f_μ
A_λ, B_λ turbulence model constants for f_λ
c_p specific heat at constant pressure
C_μ, $C_{\varepsilon 1}$, $C_{\varepsilon 2}$ turbulence model constants for velocity field
C_λ, C_{P1}, C_{P2}, C_{D1}, C_{D2} turbulence model constants for temperature field
f_μ, f_ε turbulence model functions for velocity field
f_λ, f_{D1}, f_{D2} turbulence model functions for temperature field
k turbulent kinetic energy, $\bar{u}_i\bar{u}_i/2$
$\bar{P}$ mean pressure
Pr, Pr_t molecular and turbulent Prandtl numbers
q_w wall heat flux
R time-scale ratio, τ_t/τ_u
R_h turbulence Reynolds number based on τ_m, $k(k/\varepsilon)^{-1}(\bar{t}^2/\varepsilon_t)^2/\nu$
R_t turbulence Reynolds number, $k^2/\nu\varepsilon$
Δt^2 temperature-variance difference, $\bar{t}^2-\bar{t}_w^2$
t_τ friction temperature, $q_w/\rho c_p u_\tau$
t' r.m.s. temperature, $\sqrt{(\bar{t}^2)}$
$\bar{T}$, t mean and fluctuating temperatures
$\bar{T}^+$ dimensionless temperature, $(\bar{T}_w-\bar{T})/t_\tau$
ΔT, ΔT_0, ΔT_s temperature differences, $(\bar{T}_w-\bar{T}_e)$, $(\bar{T}_{w0}-\bar{T}_e)$, $(\bar{T}_{ws}-\bar{T}_e)$
u_τ friction velocity, $(\tau_w/\rho)^{1/2}$
v fluctuating velocity component in y direction
$\bar{U}$, u mean and fluctuating velocity components in x direction
$\bar{U}_i$, u_i mean and fluctuating velocity components in x_i direction
$\bar{U}^+$ dimensionless velocity, $\bar{U}/u_\tau$
x, y coordinates in streamwise and wall-normal directions
X streamwise distance, measured from leading edge
X_c streamwise distance, measured from leading edge to the location of a step change in wall thermal condition
X_s streamwise distance, measured from a sudden change in wall thermal condition
y^+ dimensionless distance from wall, $u_\tau y/\nu$
$\overline{(\quad)}$ time mean scale.

Greek symbols

α, α_t molecular and eddy diffusivities for heat
δ boundary layer thickness
δ_0 boundary layer thickness at a sudden change in wall thermal condition
δ_T thermal layer thickness
δ_{ij} Kronecker delta
ε dissipation rate of k, $\nu(\partial u_i/\partial x_j)^2$
ε_t dissipation rate of $\bar{t}^2/2$, $\alpha(\partial\bar{t}/\partial x_j)^2$
ν, ν_t molecular and eddy viscosities
ρ density
σ_k, σ_ε, σ_h, σ_ϕ turbulence model constants for diffusion of k, ε, $\bar{t}^2/2$, and ε_t
τ, τ_w time and wall shear stress
τ_m mixed time scale, $\tau_u^l\tau_t^m$ $(l+m=1)$
τ_u, τ_t time scales of velocity and temperature fields, k/ε, $\bar{t}^2/(2\varepsilon_t)$.

Subscripts

e boundary-layer edge
w wall
wo wall upstream of a sudden change in wall thermal condition
ws wall at a point of a sudden change in wall thermal condition.

stepwise change in wall temperature, a constant heat flux followed by an adiabatic wall, and finally a constant temperature followed by an adiabatic wall.

Except for the new points, Section 2 provides only a brief presentation of the mathematical model of turbulence for velocity field. Details of a new $\bar{t}^2$–ε_t heat transfer model are provided in Section 3. Section 4 gives a short description of the numerical solution algorithm. Comparison between the proposed model results and the available experimental and full simulation data, together with the predictions from previous models, are provided in Section 5.

2. TWO-EQUATION MODEL OF TURBULENCE FOR VELOCITY FIELD

A velocity field is described with the following continuity and momentum equations

$$\frac{\partial\bar{U}_i}{\partial x_i}=0 \tag{1}$$

$$\frac{D\bar{U}_i}{D\tau}=-\frac{1}{\rho}\frac{\partial\bar{P}}{\partial x_i}+\frac{\partial}{\partial x_j}\left(\nu\frac{\partial\bar{U}_i}{\partial x_j}-\overline{u_iu_j}\right) \tag{2}$$

where $D/D\tau=\partial/\partial\tau+\bar{U}_j\partial/\partial x_j$.

In the k–ε model, the Reynolds stress $\overline{u_iu_j}$ in equation (2) can be obtained from the following set of equations

$$-\overline{u_iu_j}=\nu_t\left(\frac{\partial\bar{U}_i}{\partial x_j}+\frac{\partial\bar{U}_j}{\partial x_i}\right)-\tfrac{2}{3}\delta_{ij}k \tag{3}$$

$$\nu_t=C_\mu f_\mu\frac{k^2}{\varepsilon} \tag{4}$$

$$\frac{Dk}{D\tau}=\frac{\partial}{\partial x_j}\left[\left(\nu+\frac{\nu_t}{\sigma_k}\right)\frac{\partial k}{\partial x_j}\right]-\overline{u_iu_j}\frac{\partial\bar{U}_i}{\partial x_j}-\varepsilon \tag{5}$$

$$\frac{D\varepsilon}{D\tau} = \frac{\partial}{\partial x_j}\left[\left(\nu + \frac{\nu_t}{\sigma_\varepsilon}\right)\frac{\partial \varepsilon}{\partial x_j}\right] - C_{\varepsilon 1}\frac{\varepsilon}{k}u_i u_j \frac{\partial \bar{U}_i}{\partial x_j} - C_{\varepsilon 2} f_\varepsilon \frac{\varepsilon^2}{k}. \quad (6)$$

As indicated by Myong and Kasagi [14], and by Nagano and Tagawa [12], imposing the rigid boundary condition (i.e. no-slip) at the wall does not necessarily lead to the correct asymptotic solutions of $k \propto y^2$, $-\overline{uv} \propto y^3$, $\nu_t \propto y^3$, and $\varepsilon \propto y^0$ for $y \to 0$, unless the wall limiting behavior of turbulence is properly incorporated in a turbulence model. In the present study, we use an improved k–ε turbulence model evolved by Nagano and Tagawa [12] (referred to as the NT model), which reproduces strictly the limiting behavior of wall and free turbulence. Constants and functions of the NT model are summarized in Table 1. Note that, in the NT model, away from the wall (where the turbulence Reynolds number R_t becomes large), the relation $\nu_t \propto k^{1/2}L_e (L_e = k^{3/2}/\varepsilon)$ holds and the eddy viscosity is thereby determined by the large-scale energy-containing eddies; but close to the wall, the eddy viscosity is reduced to $\nu_t \propto k^{1/2}\eta$ ($\eta = (\nu^3/\varepsilon)^{1/4}$ is the Kolmogorov microscale) and determined by the small-scale eddies dominating mainly the dissipation process.

3. TWO-EQUATION MODEL FOR THERMAL FIELD

3.1. *Governing equations*

Using the concept of eddy diffusivity for heat α_t, the governing equations of the two-equation heat transfer model may be written (see, Nagano and Kim [8]; Nagano *et al.* [15]) as

$$\frac{D\bar{T}}{D\tau} = \frac{\partial}{\partial x_j}\left(\alpha \frac{\partial \bar{T}}{\partial x_j} - \overline{u_j t}\right) \quad (7)$$

$$-\overline{u_j t} = \alpha_t \frac{\partial \bar{T}}{\partial x_j} \quad (8)$$

$$\alpha_t = C_\lambda f_\lambda k \left(\frac{k}{\varepsilon}\right)^l \left(\frac{\overline{t^2}}{\varepsilon_t}\right)^m, \quad l+m=1 \quad (9)$$

$$\frac{D\overline{t^2}}{D\tau} = \frac{\partial}{\partial x_j}\left[\left(\alpha + \frac{\alpha_t}{\sigma_h}\right)\frac{\partial \overline{t^2}}{\partial x_j}\right] - 2\overline{u_j t}\frac{\partial \bar{T}}{\partial x_j} - 2\varepsilon_t \quad (10)$$

$$\frac{D\varepsilon_t}{D\tau} = \frac{\partial}{\partial x_j}\left[\left(\alpha + \frac{\alpha_t}{\sigma_\phi}\right)\frac{\partial \varepsilon_t}{\partial x_j}\right] - C_{P1}\frac{\varepsilon_t}{\overline{t^2}}\overline{u_j t}\frac{\partial \bar{T}}{\partial x_j}$$
$$- C_{P2}\frac{\varepsilon_t}{k}\overline{u_i u_j}\frac{\partial \bar{U}_i}{\partial x_j} - C_{D1} f_{D1}\frac{\varepsilon_t^2}{\overline{t^2}} - C_{D2} f_{D2}\frac{\varepsilon\varepsilon_t}{k}. \quad (11)$$

As a time-scale equivalent to the relative 'lifetime' of the energy-containing eddies or temperature fluctuations, we adopt the mixed time-scale $\tau_m = \tau_u^l \tau_t^m$ ($l+m=1$), where $\tau_u = k/\varepsilon$ and $\tau_t = (\overline{t^2}/2)/\varepsilon_t$ are the dynamic and scalar time-scales, respectively. Obviously, τ_m blends both thermal and mechanical contributions. The characteristic length scale (i.e. spatial extent of a fluctuating temperature) can hence be written as $L_m = k^{1/2}\tau_m$, and the eddy diffusivity for heat can be modeled as $\alpha_t \propto k^{1/2}L_m = k\tau_m$ (equation (9)). The present expression for α_t can be regarded as the generalized form for the eddy diffusivity introduced by Nagano and Kim [8]. As described later, the indices l and m are to be determined so as to satisfy the requirements for the wall limiting behavior of thermal turbulence. In the NT model for velocity field, the wall-proximity effects are incorporated mainly into the model function of f_μ. Accordingly, we reflect the near-wall effects in a thermal field on the model function of f_λ.

The optimal value of eddy diffusivity for heat α_t can be given as a function of the state of both velocity and thermal fields by solving the transport equations for k, ε, $\overline{t^2}$, and ε_t. The determination of the model constants and functions in equations (9)–(11) will be discussed later.

3.2. *Modeling of wall limiting behavior of velocity and temperature*

As mentioned above, we devise the modeling of f_λ in equation (9), which has some properties in common with f_μ in equation (4), to account for low-Reynolds-number and/or wall-proximity effects, thus, taking into account the formulation for f_μ given in Table 1, we write f_λ as follows

$$f_\lambda = \{1 - \exp(-y^+/A_\lambda)\}^2 (1 + B_\lambda/R_h^n) \quad (12)$$

where $R_h = k(k/\varepsilon)^l(\overline{t^2}/\varepsilon_t)^m/\nu$ is the turbulence Reynolds number based on the mixed time scale.

The behavior of the turbulent quantities of velocity and thermal fields near the wall can be inferred from a Taylor series expansion in terms of y, together with the continuity, momentum and energy equations, namely,

$$\bar{U}^+ = y^+ + a_1 y^{+2} + a_2 y^{+3} + \cdots$$
$$u = b_1 y + b_2 y^2 + b_3 y^3 + \cdots$$
$$v = c_1 y^2 + c_2 y^3 + \cdots$$
$$w = d_1 y + d_2 y^2 + d_3 y^3 + \cdots$$
$$k = \overline{u_i u_i}/2 = [(\overline{b_1^2} + \overline{d_1^2})/2]y^2 + (b_1\overline{b_2} + \overline{d_1 d_2})y^3 + \cdots$$

Table 1. Constants and functions in the NT model equations

C_μ	$C_{\varepsilon 1}$	$C_{\varepsilon 2}$	σ_k	σ_ε	f_μ	f_ε	A_μ	B_μ
0.09	1.45	1.9	1.4	1.3	$[1-\exp(-y^+/A_\mu)]^2 \times (1 + B_\mu/R_t^{3/4})$	$\{1-0.3\exp[-(R_t/6.5)^2]\} \times [1-\exp(-y^+/6)]^2$	26	4.1

$$\overline{uv} = \overline{b_1 c_1} y^3 + (\overline{b_1 c_2} + \overline{c_1 b_2}) y^4 + \cdots$$
$$\varepsilon_w = \nu(\partial^2 k/\partial y^2)_w = \nu(\overline{b_1^2} + \overline{d_1^2})$$
$$\bar{T}^+ = Pry^+ + g_1 y^{+2} + g_2 y^{+3} + \cdots$$
$$t = t_w + h_1 y + h_2 y^2 + \cdots$$
$$\overline{t^2} = \overline{t_w^2} + (h_1^2 + 2\overline{h_2 t_w}) y^2 + \cdots$$
$$\overline{vt} = \overline{c_1 t_w} y^2 + (\overline{c_2 t_w} + \overline{c_1 h_1}) y^3 + \cdots$$
$$\varepsilon_{tw} = \alpha[\partial^2(t^2/2)/\partial y^2]_w = \alpha(h_1^2 + 2\overline{h_2 t_w}) \quad (13)$$

In equation (13), considering a correspondence between k and $\overline{t^2}$ profiles near the wall, a smooth change in temperature variance $\overline{t^2}$ in the immediate vicinity of the wall is assumed, i.e. $(\partial \overline{t^2}/\partial y)_w = 0$, which is exact in the cases of both uniform wall temperature and uniform wall heat flux. From equation (13), in the vicinity of the wall, we obtain the following relations: $\bar{U}^+ = y^+$, $u \propto y$, $v \propto y^2$, $w \propto y$, $\bar{T}^+ = Pry^+$, and $t \propto y^{p/2}$ (where, $p = 2$: without wall-temperature, t_w, fluctuations; $p = 0$: with t_w fluctuations). These asymptotic relations provide the representation for the wall limiting behavior of turbulence given as: $k \propto y^2$, $-\overline{uv} \propto y^3$, $\varepsilon \propto y^0$, $\overline{t^2} \propto y^p$, $\overline{vt} \propto y^{2+p/2}$ and $\varepsilon_t \propto y^0$, thus, substituting these asymptotic solutions for equations (9) and (12), we obtain

$$\alpha_t \propto y^{4-2n+(1-n)(pm+2l)}. \quad (14)$$

Note that, as seen from equation (8), $\overline{vt}$ and α_t have the same power for y near the wall. Consequently, from the wall limiting behavior of turbulence, we have the following two regimes according to the wall thermal conditions

$$\begin{aligned} &\alpha_t \propto y^3 \quad \text{for } p = 2 \quad \text{(without } t_w \text{ fluctuations)} \\ &\alpha_t \propto y^2 \quad \text{for } p = 0 \quad \text{(with } t_w \text{ fluctuations).} \end{aligned} \quad (15)$$

To satisfy the above requirements consistently, equation (14) yields: $n = 3/4$, $l = -1$, and $m = 2$.

From the foregoing consideration, the eddy diffusivity for heat α_t, which takes into account the near-wall behavior of thermal turbulence, can be written as

$$\alpha_t = C_\lambda f_\lambda k \left(\frac{k}{\varepsilon}\right)^{-1} \left(\frac{\overline{t^2}}{\varepsilon_t}\right)^2 = C_\lambda f_\lambda \frac{k^2}{\varepsilon}(2R)^2 \quad (16)$$

where

$$f_\lambda = [1 - \exp(-y^+/A_\lambda)]^2(1 + B_\lambda/R_h^{3/4}) \quad (17)$$
$$R_h = k(k/\varepsilon)^{-1}(\overline{t^2}/\varepsilon_t)^2/\nu = R_t(2R)^2. \quad (18)$$

Here $R = \tau_t/\tau_u = (\overline{t^2}/2\varepsilon_t)/(k/\varepsilon)$ is the thermal–mechanical time-scale ratio. As seen from equation (18), the turbulence Reynolds number, R_h, based on the mixed time scale is directly linked to the hydrodynamic turbulence Reynolds number $R_t = k^2/\nu\varepsilon$ through the time-scale ratio R. In particular, when the velocity and thermal fields are in local equilibrium, R becomes nearly 0.5 (Béguier *et al.* [16]), and hence $\alpha_t = C_\lambda f_\lambda k^2/\varepsilon$, $R_h = R_t$, and $Pr_t = C_\mu/C_\lambda$. It should also be mentioned here that, in the region away from the wall, the present formulation for α_t given by equation (16) is compatible with a statistical model developed by Yoshizawa [17].

On the other hand, from equation (11), the molecular diffusion term balances with the dissipation terms at $y = 0$:

$$\alpha \frac{\partial^2 \varepsilon_t}{\partial y^2} = C_{D1} f_{D1} \frac{\varepsilon_t^2}{\overline{t^2}} + C_{D2} f_{D2} \frac{\varepsilon\varepsilon_t}{k}. \quad (19)$$

Considering the limiting behavior of wall turbulence, $f_{D2} \propto y^2$ and $f_{D1} \propto y^2$ (without t_w fluctuations) or $f_{D1} \propto y^n$ where $n > 0$ (with t_w fluctuations) are required to satisfy equation (19). In free turbulence, as described in the next section (see equation (29)), the limiting behavior requires

$$C_{D2} f_{D2} = C_{\varepsilon 2} f_\varepsilon - 1. \quad (20)$$

In the present model, the following equations are thus proposed to meet the requirements for both wall and free turbulence

$$f_{D1} = [1 - \exp(-y^+/B_{D1})]^2 \quad (21)$$
$$f_{D2} = (1/C_{D2})(C_{\varepsilon 2} f_\varepsilon - 1)[1 - \exp(-y^+/B_{D2})]^2 \quad (22)$$

with $f_\varepsilon = 1 - 0.3 \exp[-(R_t/6.5)^2]$.

3.3. *Model constants*

The constants appearing in the present two-equation heat transfer model are determined as follows. Firstly, we specify a value of C_λ in equation (16) defining the eddy diffusivity for heat α_t. In the log-law region where the molecular diffusion is negligible, i.e. $f_\mu = f_\lambda = 1$, C_λ may be given from equations (4) and (16), together with the turbulent Prandtl number $Pr_t = \nu_t/\alpha_t$, by

$$C_\lambda = C_\mu/[Pr_t(2R)^2] \quad (23)$$

thus, substituting the typical values of $C_\mu = 0.09$, $R = 0.5$, and $Pr_t = 0.9$ (Nagano and Kim [8]), we obtain $C_\lambda = 0.10$.

We determine the constants C_{D1} and C_{D2} in the ε_t equation (11) from the decay law of homogeneous turbulence. In a homogeneous decaying turbulent flow, equations (5), (6), (10) and (11) become simply

$$\bar{U} \frac{\mathrm{d}k}{\mathrm{d}x} = -\varepsilon \quad (24)$$

$$\bar{U} \frac{\mathrm{d}\varepsilon}{\mathrm{d}x} = -C_{\varepsilon 2} f_\varepsilon \frac{\varepsilon^2}{k} \quad (25)$$

$$\bar{U} \frac{\mathrm{d}t^2}{\mathrm{d}x} = -2\varepsilon_t \quad (26)$$

$$\bar{U} \frac{\mathrm{d}\varepsilon_t}{\mathrm{d}x} = -C_{D1} f_{D1} \frac{\varepsilon_t^2}{\overline{t^2}} - C_{D2} f_{D2} \frac{\varepsilon\varepsilon_t}{k} \quad (27)$$

where the x axis is taken in the flow direction. On the other hand, it is known that the time-scale ratio $R = (\overline{t^2}/2\varepsilon_t)/(k/\varepsilon)$ does not change in the flow direction in homogeneous grid-generated turbulence (Newman *et*

al. [18], Warhaft and Lumley [19]), thus, rewriting equation (27) in terms of R and substituting equations (24)–(26) into this equation, we obtain

$$\bar{U}\frac{\mathrm{d}\varepsilon_t}{\mathrm{d}x} = \frac{1}{2R}\left(\frac{\varepsilon^2\overline{t^2}}{k^2} - C_{\varepsilon 2}f_\varepsilon\frac{\varepsilon^2\overline{t^2}}{k^2} - 2\frac{\varepsilon\varepsilon_t}{k}\right)$$

$$= -2\frac{\varepsilon_t^2}{\overline{t^2}} - (C_{\varepsilon 2}f_\varepsilon - 1)\frac{\varepsilon\varepsilon_t}{k}. \quad (28)$$

Equations (27) and (28) give the following relations

$$C_{D1}f_{D1} = 2$$

$$C_{D2}f_{D2} = C_{\varepsilon 2}f_\varepsilon - 1. \quad (29)$$

Equation (29) is also valid for the initial period ($f_\varepsilon = f_{D1} = f_{D2} = 1$) in decaying turbulent flows, and hence we have $C_{D1} = 2$ and $C_{D2} = C_{\varepsilon 2} - 1 = 0.9$.

The constants σ_h and σ_ϕ for the turbulent diffusion terms in the $\overline{t^2}$ and ε_t equation, (10) and (11), are assigned the same value of 1.0. This is consistent with the NK model.

The model constants C_{P1} and C_{P2} for the production terms in the ε_t-equation (11) are determined by considering the characteristics of the log-law region (constant stress–heat-flux layer) in wall turbulence. In this region, the convection terms in the transport equations for k, ε, $\overline{t^2}$, and ε_t can all be ignored, and the production terms for k and $\overline{t^2}$ balance with the respective dissipation terms, thus, with equation (16), rewriting equation (11) gives

$$\frac{C_\lambda}{\sigma_\phi}\frac{\partial}{\partial y}\left(\frac{k^2}{\varepsilon}(2R)^2\frac{\partial\varepsilon_t}{\partial y}\right) - C_{P1}\frac{\varepsilon_t}{\overline{t^2}}\overline{vt}\frac{\partial\bar{T}}{\partial y}$$

$$- C_{P2}\frac{\varepsilon_t}{k}\overline{uv}\frac{\partial\bar{U}}{\partial y} - C_{D1}\frac{\varepsilon_t^2}{\overline{t^2}} - C_{D2}\frac{\varepsilon\varepsilon_t}{k} = 0. \quad (30)$$

With the above-mentioned characteristics of constant stress–heat-flux layer, the following relation is obtained from equation (30)

$$C_{P2} = (C_{D1} - C_{P1})/2R + C_{D2} - (\kappa^2/Pr_t)/\sigma_\phi C_\mu^{1/2} \quad (31)$$

where κ is the von Kármán constant. Equation (31) is similar to the well-known relation in the k–ε model given by

$$C_{\varepsilon 1} = C_{\varepsilon 2} - \kappa^2/\sigma_\varepsilon C_\mu^{1/2}. \quad (32)$$

The value of $C_{P2} = 0.64$ is then specified if we substitute the foregoing values of C_{D1}, C_{D2}, R, Pr_t, and C_μ for equation (31), together with $\kappa = 0.39$–0.41 and $C_{P1} = 1.70$ which is determined on the basis of computer optimization. Note that the present value of $C_{P1} = 1.70$ is very close to the NK model constant, $C_{P1} = 1.80$. (Recently, Jones and Musonge [20] developed the transport equation for ε_t similar to equation (11) and assigned the value of $C_{P1} = 1.70$ and $C_{P2} = 1.40$.)

The constants A_λ and B_λ in equation (17) are set to $A_\lambda = A_\mu/Pr^{1/2}$ and $B_\lambda = 3.4$, after consideration of the wall-proximity and Prandtl number effects described by Nagano and Kim [8]. The constants B_{D1} and B_{D2} in equations (21) and (22), on the other hand, are assigned to $B_{D1} = 5.8$ and $B_{D2} = 6.0$ in the light of the constant for f_ε in Table 1.

The model constants and functions of the proposed two-equation heat transfer model are summarized in Table 2.

4. NUMERICAL SCHEME AND BOUNDARY CONDITIONS

Full details of the present numerical method of solution are given in Nagano and Kim [8] and Nagano and Tagawa [12]. The numerical technique used is the well tested Keller's Box method (Bradshaw *et al.* [21]). Non-uniform grids in the normal direction with shorter steps close to the wall and longer steps away from the wall are usually employed for the calculation of turbulent boundary layers due to the large gradients near the surface of the body [22]. There are different techniques for constructing variable grid spacing in the direction normal to a solid wall as discussed in detail by Cebeci *et al.* [23], and Blottner [24, 25]. The following non-uniform grid across the layer is thus employed

$$y_j = \Delta y_1(K^j - 1)/(K - 1) \quad (33)$$

where Δy_1, the length of the first step, and K, the ratio of any two successive steps, are chosen as 10^{-5} and 1.03, respectively. To obtain grid-independent solutions, 201 cross-stream grid points were used. The first grid point was normally located well into the viscous sublayer, i.e. $y^+ < 0.03$. To confirm the numerical accuracy, the cross-stream grid interval was cut in half for the uniform wall temperature case. No significant differences were seen in the results. The maximum streamwise step-size was restricted to a sublayer thickness, i.e. $\Delta x^+ < 1$.

The boundary conditions at the wall ($y = 0$) for a velocity field are: $\bar{U} = k = 0$ and $\varepsilon_w = \nu(\partial^2 k/\partial y^2)_w$ or equivalently $\varepsilon_w = 2\nu(\partial k^{1/2}/\partial y)_w^2$ as can be seen from equation (13). The latter boundary condition for ε at the wall provides much stabler computations and hence is used in the present model. For a thermal field, on the other hand, the wall boundary conditions are: $\bar{T} = \bar{T}_w$ and $\overline{t^2} = 0$ for a uniform wall temperature,

Table 2. Constants and functions in the proposed model equations

C_λ	C_{P1}	C_{P2}	C_{D1}	C_{D2}	σ_h	σ_ϕ	f_λ	f_{D1}	f_{D2}	A_λ	B_λ
0.1	1.7	0.64	2.0	0.9	1.0	1.0	$[1-\exp(-y^+/A_\lambda)]^2 \times (1 + B_\lambda/R_h^{3/4})$	$[1-\exp(-y^+/5.8)]^2$	$(1/C_{D2})(C_{\varepsilon 2}f_\varepsilon - 1) \times [1-\exp(-y^+/6)]^2$	$26/Pr^{1/2}$	3.4

$\alpha(\partial\bar{T}/\partial y)_w = -q_w/\rho c_p$ and $(\partial\overline{t^2}/\partial y)_w = 0$ for a uniform wall heat flux, and $(\partial\bar{T}/\partial y)_w = 0$ and $(\partial\overline{t^2}/\partial y)_w = 0$ for an adiabatic wall. Note that the temperature-variance dissipation rate balances with the molecular diffusion at the wall, so that $\varepsilon_{tw} = \alpha(\partial^2(\overline{t^2}/2)/\partial y^2)_w$ holds, irrespective of wall thermal conditions. Again, it can be seen from equation (13) that this boundary condition for ε_t is identical to the expression: $\varepsilon_{tw} = \alpha(\partial\sqrt{(\Delta t^2)}/\partial y)_w^2$ with $\Delta t^2 = \overline{t^2}(x, y, z) - \overline{t^2}(x, 0, z) = \overline{t^2} - t_w^2$, which provides stabler computations and thus is used in the present model. At the free stream, the boundary conditions are $\bar{U} = \bar{U}_e$, $\bar{T} = \bar{T}_e$, and $k = \varepsilon = \overline{t^2} = \varepsilon_t = 0$.

The criterion for convergence is

$$\max|Y^{(i+1)} - Y^{(i)}|/\max|Y^{(i)}| < 10^{-5} \qquad (34)$$

where $Y = \partial Z/\partial y(Z: \bar{U}, k, \varepsilon, \bar{T}, \overline{t^2}$, and $\varepsilon_t)$, and i denotes the number of iterations. The computations were performed on a TITAN 3000 computer.

5. RESULTS AND DISCUSSION

As described in the preceding section, there are two types of wall limiting behavior for turbulence quantities in a thermal field, both of which depend on the imposed wall thermal conditions. To verify the adequacy of the present model, first we have analyzed the thermal fields in a boundary layer (air flow) with two typical boundary conditions, i.e. with a uniform wall temperature and with a uniform wall heat flux. Next, the proposed model was tested by application to boundary layers with other three different thermal fields; namely, a step change in wall temperature, a constant heat flux followed by an adiabatic wall, and a constant temperature followed by an adiabatic wall.

5.1. *Uniform temperature and uniform heat-flux walls*

In Fig. 1, comparison is made between the experimental temperature profiles in the turbulent boundary layers under two different wall thermal conditions (Žukauskas and Šlančiauskas [26], Gibson *et al.* [27], and Antonia *et al.* [28]) and the present predictions. The model predictions by Launder and Samaraweera [29] are also shown for comparison. It can be seen that the present model gives good predictions for both the uniform wall temperature and uniform wall heat-flux conditions, while the predictions of Launder and Samaraweera, who used a second-moment closure model, in the outer region of a boundary layer are less satisfactory. Predictions for temperature close to the wall were not presented in their paper [29].

Figure 2 shows the near-wall profiles of temperature variance t^2. For a uniform wall temperature condition, the present model predicts the relation $\overline{t^2}/t_\tau^2 = 0.03y^{+2}$ in the vicinity of the wall, thus satisfying the required wall limiting behavior. For a uniform wall heat-flux condition, on the other hand, the predicted $\overline{t^2}$ distribution approaches a constant non-zero value for $y \to 0$, which is also consistent with the outcome from the Taylor series expansion analysis. The results of direct numerical simulations (DNS) for channel flows with a uniform wall temperature (Kim and Moin [30]) and with a quasi-uniform wall heat flux, i.e. $\partial\bar{T}_w/\partial x$ = constant and $\overline{t_w^2} = 0$ (Kasagi *et al.* [31]) are included in Fig. 2 for comparison, though the relevant Reynolds numbers are much lower than those in the present predictions. Both DNS results provide solutions similar to the present ones. Included here are the experimental data of Antonia *et al.* [28] (q_w = constant) and Subramanian and Antonia [32] (q_w = constant). It can be seen that, good agreement is obtained between the present predictions and the experimental data.

As discussed previously, the turbulent heat flux $\overline{vt}$ needs to satisfy the wall limiting behavior of $\overline{vt} \propto y^3$ for a uniform wall-temperature case and $\overline{vt} \propto y^2$ for a uniform wall heat-flux case. As shown in Fig. 3, the present model reproduces these relations accurately and gives good agreement with the measurements of Antonia *et al.* [28].

In the present model, we use the physically strict relation $\varepsilon_{tw} = \alpha(\partial\sqrt{(\Delta\overline{t^2})}/\partial y)_w^2$ as a wall boundary condition, thus, in Fig. 4, the near-wall distributions of ε_t predicted by the present model are compared with both the result of the DNS of Kasagi *et al.* [31] and the measurement of Krishnamoorthy and Antonia [33]. The present results for constant wall temperature and constant wall heat flux, are identical except very close to the wall where different wall boundary conditions are imposed. The present results are in good agreement with the DNS data of Kasagi *et al.* for

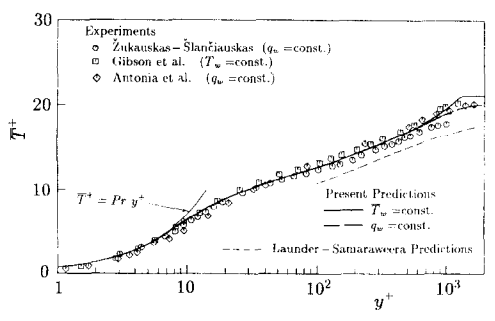

FIG. 1. Mean temperature profiles in a flat-plate boundary layer.

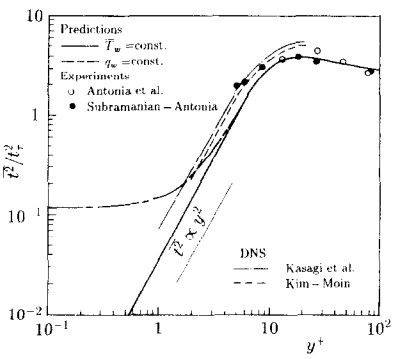

FIG. 2. Near-wall behavior of temperature variance.

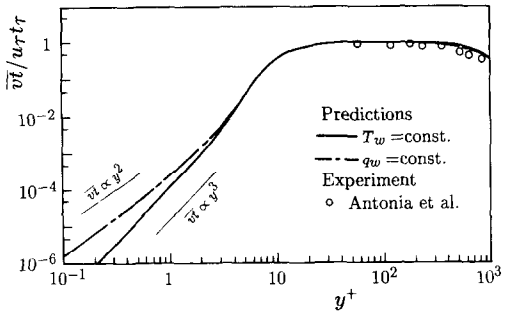

FIG. 3. Near-wall behavior of turbulent heat flux.

$y^+ > 20$. It can also be seen from the figure that the proposed model provides a reasonable overall consensus with the experimental data of Krishnamoorthy and Antonia [33]. In the k–ε model, it is well known that the model prediction gives values lower than the DNS [34, 35]. The difference between the results of the DNS and the present model near the wall would be attributed to the similar reasons found in the k–ε model, although the detailed discussion is left for a future study.

5.2. *Step change in wall temperature*

To further verify the effectiveness of the present model for calculating various kinds of turbulent thermal fields, the prediction of mean temperature profiles for a constant wall temperature ($\bar{T}_w = \bar{T}_e + 16°C$) followed by another constant wall temperature ($\bar{T}_w = \bar{T}_e$) are shown in Fig. 5. Also, included here are the experimental data of Charnay *et al.* [36] and the calculations of Browne and Antonia [37] at the same streamwise locations. It must be mentioned that Browne and Antonia used a two-equation model of turbulence and a turbulent heat-flux equation model in their calculations. As is clearly seen, the present predictions are in good agreement with the measurements while the results of Browne and Antonia give considerable overpredictions.

5.3. *Constant heat flux followed by adiabatic wall*

The test case of a constant heat flux followed by an adiabatic wall is also very suitable for assessing the

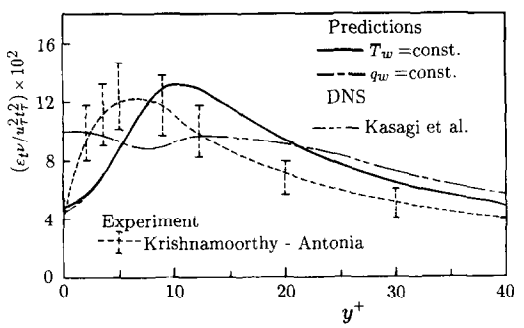

FIG. 4. Comparison of the model results for the dissipation rate of temperature variance with the measurements of Krishnamoorthy and Antonia [33].

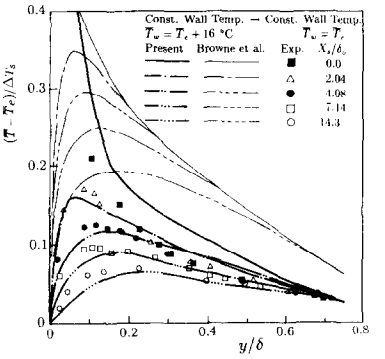

FIG. 5. Comparison of the predicted mean temperature profiles with the measurements of Charnay *et al.* [36].

performance of the model. Figure 6 shows a comparison between the present results and both the measurements of Subramanian and Antonia [38] (as reported in Browne and Antonia [37]) and the calculated results of Browne and Antonia [37] for the mean temperature profiles across the boundary layer. Again, for this test case, the present results are seen to be in good agreement with the experimental data; however, rather poor agreement is obtained between the predicted results of Browne and Antonia and the measurements as shown in Fig. 6.

The distributions of r.m.s. temperature predicted from the proposed model are shown in Fig. 7, compared with the measurements of Subramanian and Antonia [38]. The general level of agreement with the experimental values at all locations is found to be very good.

5.4. *Constant temperature followed by adiabatic wall*

The last test case for which calculations have been performed is concerned with the thermal fields in a boundary layer along a constant wall temperature followed by an adiabatic wall. Figure 8 shows a comparison of the predicted results with the measured values (Reynolds *et al.* [39]) of temperature differences between the wall and the free stream. Figure 8 also includes the wall-temperature distribution downstream of the discontinuity in heat flux predicted by

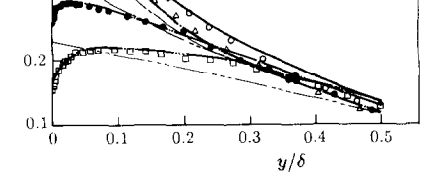

FIG. 6. Comparison of the predicted mean temperature profiles with the measurements of Subramanian and Antonia [38].

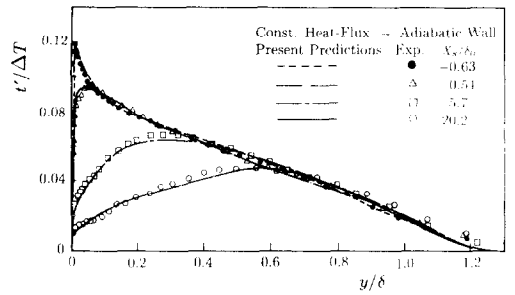

FIG. 7. Comparison between the calculated r.m.s. temperature profiles and the measurements of Subramanian and Antonia [38].

the integral analysis of Reynolds *et al.* [39] and of Rubesin [40]. It can be seen that the present model gives results similar to the integral-equation predictions of Rubesin and in acceptable agreement with the measurements.

Now that the forgoing test cases have validated the performace of the present model, we will look in more detail at the turbulent thermal field in the last test case. The measurements are not available for turbulence statistics; thus, the model predictions are the only means to understand the phenomena. In what follows, turbulence quantities related to temperature are normalized by $\Delta T_0 (= \bar{T}_{w0} - \bar{T}_e)$ and the streamwise location X by X_c which is a distance from a leading edge to the location of a step change in surface thermal condition.

Variations in the temperature variance $\overline{t^2}$ and turbulent heat-flux $\overline{vt}$ profiles in the thermal layer upstream and downstream of a sudden change in surface condition (i.e. constant temperature-adiabatic wall) are shown in Figs. 9 and 10, respectively. It can be seen that the temperature variance $\overline{t^2}$ peaks near the wall in the upstream region ($X/X_c < 1$); however, in the downstream region ($X/X_c > 1$) where there is no heat input from the wall, $\overline{t^2}$ decreases with increasing X and a maximum point moves outward towards the edge of the thermal layer. This means that, downstream of the discontinuity in wall thermal condition, the generation of $\overline{t^2}$, which mainly occurs in the wall region of the heated flow, deteriorates and the diffusion of $\overline{t^2}$ from the wall region to the outer layer becomes predominant, thus gradually thickening the thermal-layer thickness. From Fig. 10, it is seen that almost the same phenomenon occurs in the decaying

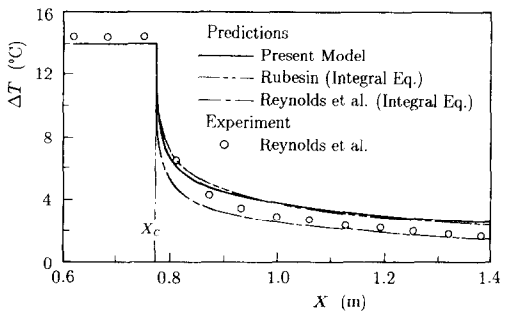

FIG. 8. Comparison of the predicted variation of wall temperatures with the measurements of Reynolds *et al.* [39].

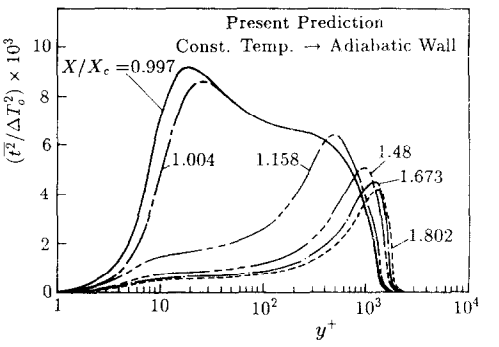

FIG. 9. Variation of temperature variance for constant temperature-adiabatic wall.

region of $\overline{vt}$. It is also worth noting that the decay process is slow in a wall turbulent thermal field.

The variation of ε_t with X shown in Fig. 11 discloses an important feature of a decaying thermal layer. The decay of the dissipation of $\overline{t^2}$ in the turbulent boundary layer on an adiabatic wall is very rapid. This, in turn, brings about the slow decay of temperature fluctuations as shown in Fig. 9. The cause and effect may be explained by the resultant temperature profiles shown in the next figure.

Figure 12 shows how a wall turbulent thermal layer decays when heat input is cut off. A very abrupt decrease in mean fluid temperature occurs in the wall region so as to satisfy the no heat-input condition, i.e. $(\partial \bar{T}/\partial y)_w = 0$. Within a short distance from the discontinuity point, the profile of mean temperature becomes uniform over most of the thermal layer. The generation of both $\overline{t^2}$ and ε_t through a mean temperature gradient thus disappears. This is the reason why the values of $\overline{t^2}$ and ε_t decrease sharply in the wall

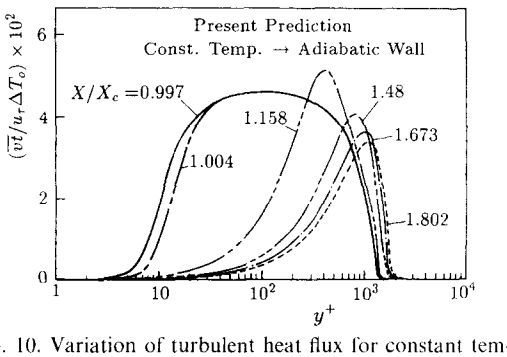

FIG. 10. Variation of turbulent heat flux for constant temperature-adiabatic wall.

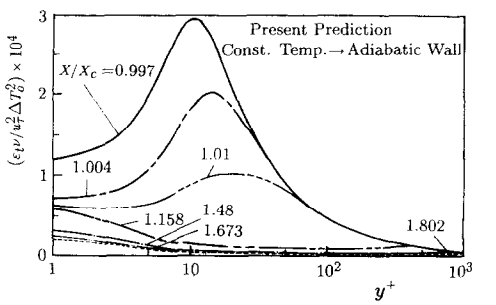

FIG. 11. Variation of dissipation rate of temperature variance for constant temperature-adiabatic wall.

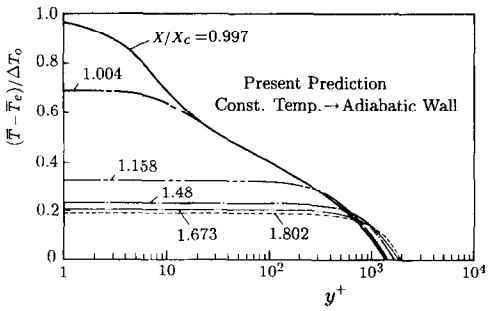

FIG. 12. Mean temperature profiles for constant temperature-adiabatic wall.

region as shown in Figs. 9 and 11. Consequently, a key factor which controls the decaying thermal turbulence is the turbulent diffusion. Although the experimental documentation is needed, these results demonstrate the usefulness of the proposed two-equation heat transfer model to investigate the structure of thermal turbulence.

In this study, we have tested the proposed heat transfer model under various kinds of wall thermal conditions. Dependency on a molecular Prandtl number is not, however, tested systematically, hence, in the next paper, we will report on this subject.

6. CONCLUSIONS

The main conclusions of the present investigation can be summarized as follows.

(i) The model developed in this work reproduces the correct wall limiting behavior of thermal fields which changes with the wall thermal conditions.

(ii) In comparison with second-moment, heat-flux equation models, the present model can be applicable to turbulent thermal fields with different thermal wall boundary conditions. The previous heat-flux models failed to predict the near-wall asymptotic behavior in a simple case of wall thermal boundary condition as reported by Launder and Samaraweera [29] and provided rather unsatisfactory predictions of turbulent thermal quantities [37]. It is established, therefore, with reinforced evidence, that the performance of the proposed model is much better than the previous models.

(iii) The proposed heat-transfer model discovers novel features of the decaying process of turbulent thermal-field quantities in a boundary layer and adds a reasonable comprehension about the scalar transport mechanisms in this physical phenomenon.

REFERENCES

1. A. J. Reynolds, The prediction of turbulent Prandtl and Schmidt numbers, *Int. J. Heat Mass Transfer* **18,** 1055–1069 (1975).
2. T. Cebeci, A model for eddy conductivity and turbulent Prandtl number, *J. Heat Transfer* **95,** 227–234 (1973).
3. R. A. Antonia, Behaviour of the turbulent Prandtl number near the wall, *Int. J. Heat Mass Transfer* **23,** 906–908 (1980).
4. Y. Nagano and M. Tagawa, Statistical characteristics of wall turbulence with a passive scalar, *J. Fluid Mech.* **196,** 157–185 (1988).
5. Y. Nagano and M. Tagawa, A structural turbulence model for triple products of velocity and scalar, *J. Fluid Mech.* **215,** 639–657 (1990).
6. Y. Nagano and M. Tagawa, Turbulence model for triple velocity and scalar correlations. In *Turbulent Shear Flows 7* (Edited by F. Durst *et al.*), pp. 47–62. Springer, Berlin (1991).
7. W. Rodi, *Turbulence Models and Their Application in Hydraulics—A State of the Art Review*, 2nd Edn. International Association for Hydraulic Research-Publication, Delft (1984).
8. Y. Nagano and C. Kim, A two-equation model for heat transport in wall turbulent shear flows, *J. Heat Transfer* **110,** 583–589 (1988).
9. E. G. Tulapurkara, R. A. Antonia and L. W. B. Browne, Optimisation of a $\overline{\theta^2}-\varepsilon_\theta$ model for a turbulent far wake, *Proc. 7th Symp. on Turbulent Shear Flows*, Stanford University, pp. 29.2.1–29.2.6 (1989).
10. K.-L. Tzuoo, J. H. Ferziger and S. J. Kline, Zonal models of turbulence and their application to free shear flows, Tech. Rep. No. TF-27, Dept. Mech. Engng, Stanford University (1986).
11. E. G. Tulapurkara, R. A. Antonia and L. W. B. Browne, Optimisation of the k–ε model for a turbulent far-wake, *J. Aero. Soc. India* **42,** 221–228 (1990).
12. Y. Nagano and M. Tagawa, An improved k–ε model for boundary layer flows, *J. Fluids Engng* **112,** 33–39 (1990).
13. Y. Nagano and M. Hishida, Improved form of the k–ε model for wall turbulent shear flows, *J. Fluids Engng* **109,** 156–160 (1987).
14. H. K. Myong and N. Kasagi, A new approach to the improvement of k–ε turbulence model for wall-bounded shear flows, *JSME Int. J.* **33,** 63–72 (1990).
15. Y. Nagano, M. Tagawa and T. Tsuji, An improved two-equation heat transfer model for wall turbulent shear flows, *Proc. ASME–JSME Thermal Engng Joint Conf.*, Reno, Nevada (Edited by J. Lloyd and Y. Kurosaki), Vol. 3, pp. 233–240 (1991).
16. C. Béguier, I. Dekeyser and B. E. Launder, Ratio of scalar and velocity dissipation time scales in shear flow turbulence, *Physics Fluids* **21,** 307–310 (1978).
17. A. Yoshizawa, Statistical modelling of passive-scalar diffusion in turbulent shear flows, *J. Fluid Mech.* **195,** 541–555 (1988).
18. G. R. Newman, B. E. Launder and J. L. Lumley, Modelling the behaviour of homogeneous scalar turbulence, *J. Fluid Mech.* **111,** 217–232 (1981).
19. Z. Warhaft and J. L. Lumley, An experimental study of the decay of temperature fluctuations in grid-generated turbulence, *J. Fluid Mech.* **88,** 659–684 (1978).
20. W. P. Jones and P. Musonge, Closure of the Reynolds stress and scalar flux equations, *Physics Fluids* **31,** 3589–3604 (1988).
21. P. Bradshaw, T. Cebeci and J. H. Whitelaw, *Engineering Calculation Methods for Turbulent Flow*. Academic Press, London (1981).
22. M. S. Youssef, Predictions of incompressible turbulent boundary layers under different adverse pressure gradients, M.S. Thesis, Dept. Mech. Engng, Assuit University, Egypt (1989).
23. T. Cebeci, A. M. O. Smith and G. Mosinskis, Calculation of compressible adiabatic turbulent boundary layers, *AIAA J.* **8,** 1974–1982 (1970).
24. F. G. Blottner, Variable grid scheme applied to turbulent boundary layers, *Comput. Meth. Appl. Mech. Engng* **4,** 179–194 (1974).
25. F. G. Blottner, Variable grid scheme for discontinuous grid spacing and derivatives, *Comput. Fluids* **8,** 421–434 (1980).
26. A. Žukauskas and A. Šlančiauskas, *Heat Transfer in*

Turbulent Fluid Flows (Edited by J. Karni). Hemisphere, New York (1987).
27. M. M. Gibson, C. A. Verriopoulos and Y. Nagano, Measurements in the heated turbulent boundary layer on a mildly curved convex surface. In *Turbulent Shear Flows 3* (Edited by L. J. S. Bradbury *et al.*), pp. 80–89. Springer, Berlin (1982).
28. R. A. Antonia, H. Q. Danh and A. Prabhu, Response of a turbulent boundary layer to a step change in surface heat flux, *J. Fluid Mech.* **80,** 153–177 (1977).
29. B. E. Launder and D. S. A. Samaraweera, Application of a second-moment turbulence closure to heat and mass transport in thin shear flows—I. Two-dimensional transport, *Int. J. Heat Mass Transfer* **22,** 1631–1643 (1979).
30. J. Kim and P. Moin, Transport of passive scalars in a turbulent channel flow. In *Turbulent Shear Flows 6* (Edited by J. C. André *et al.*), pp. 85–96. Springer, Berlin (1989).
31. N. Kasagi, Y. Tomita and A. Kuroda, Direct numerical simulation of the passive scalar field in a two dimensional turbulent channel flow, *Proc. ASME JSME Thermal Engng Joint Conf.*, Reno, Nevada (Edited by J. Lloyd and Y. Kurosaki), Vol. 3, pp. 175–182 (1991).
32. C. S. Subramanian and R. A. Antonia, Effect of Reynolds number on a slightly heated turbulent boundary layer, *Int. J. Heat Mass Transfer* **24,** 1833–1846 (1981).
33. L. V. Krishnamoorthy and R. A. Antonia, Temperature-dissipation measurements in a turbulent boundary layer, *J. Fluid Mech.* **176,** 265–281 (1987).
34. N. N. Mansour, J. Kim and P. Moin, Near-wall k–ε turbulence modeling, *AIAA J.* **27,** 1068–1073 (1989).
35. B. E. Launder and D. P. Tselepidakis, Contribution to the second-moment modeling of sublayer turbulent transport. In *Near-Wall Turbulence* (Edited by S. J. Kline and N. H. Afgan), pp. 818–833. Hemisphere, New York (1990).
36. G. Charnay, J. P. Schon, E. Alcaraz and J. Mathieu, Thermal characteristics of a turbulent boundary layer with an inversion of wall heat flux. In *Turbulent Shear Flows 1* (Edited by F. Durst *et al.*), pp. 104–118. Springer, Berlin (1979).
37. L. W. B. Browne and R. A. Antonia, Calculation of a turbulent boundary layer downstream of a sudden decrease in surface heat flux or wall temperature, *Proc. 3rd Symp. on Turbulent Shear Flows*, University of California, Davis, pp. 10.18–10.22 (1981).
38. C. S. Subramanian and R. A. Antonia, Response of a turbulent boundary layer to a sudden decrease in wall heat flux, *Int. J. Heat Mass Transfer* **24,** 1641–1647 (1981).
39. W. C. Reynolds, W. M. Kays and S. J. Kline, Heat transfer in the turbulent incompressible boundary layer, III—Arbitrary wall temperature and heat flux, NASA MEMO. 12-3-58W (1958).
40. M. W. Rubesin, The effect of an arbitrary surface temperature variation along a flat plate on the convective heat transfer in an incompressible turbulent boundary layer, NACA TN 2345 (1951).

MODELE A DEUX EQUATIONS POUR CALCULER LES CHAMPS THERMIQUES TURBULENTS DANS DES CONDITIONS THERMIQUES ARBITRAIRES A LA PAROI

Résumé—On présente un nouveau modèle $\overline{t^2}$–ε_t avec une prédiction précise des champs turbulents thermique de paroi. Ce modèle reproduit correctement le comportement limite à la paroi de la vitesse et de la température dans des conditions thermiques pariétales arbitraires. On fait l'évaluation des constantes et des fonctions du modèle pour généraliser l'applicabilité du modèle $\overline{t^2}$–ε_t. Celui-ci est testé avec cinq champs thermiques différents typiques que l'on rencontre souvent dans les applications pratiques. Les résultats sont comparés avec les données expérimentales disponibles et aussi avec les prédictions de modèles antérieurs. On montre que le présent modèle convient mieux que les autres déjà connus.

EIN ZWEIGLEICHUNGSMODELL FÜR DEN WÄRMEÜBERGANG IN EINEM TURBULENTEN STRÖMUNGSFELD BEI BELIEBIGEN THERMISCHEN WANDBEDINGUNGEN

Zusammenfassung—Es wird ein neues Modell vom Typ $\overline{t^2}$–ε_t für den Wärmeübergang vorgestellt, was eine genaue Berechnung des wandnahen turbulenten Temperaturfeldes erlaubt. Das vorgeschlagene Modell bildet das korrekte Verhalten von Geschwindigkeit und Temperatur an der begrenzenden Wand bei beliebigen thermischen Wandbedingungen nach. Für eine allgemeine Anwendbarkeit wird eine Bewertung der Modellkonstanten und -funktionen vorgenommen. Das vorgeschlagene Modell wird anhand von fünf typischen thermischen Feldern überprüft, die oft bei technischen Anwendungen in turbulenten wandnahen Scherströmungen auftreten. Die Modellergebnisse werden mit verfügbaren Versuchsergebnissen sowie mit Ergebnissen aus vollständigen Simulationen und mit Ergebnissen aus bisher gebräuchlichen Modellen verglichen. Es zeigt sich, daß das vorgestellte Modell besser als die seither gebräuchlichen Modelle arbeitet.

ДВУХПАРАМЕТРИЧЕСКАЯ МОДЕЛЬ ТЕПЛОПЕРЕНОСА ДЛЯ ОПРЕДЕЛЕНИЯ ТУРБУЛЕНТНЫХ ТЕПЛОВЫХ ПОЛЕЙ ПРИ ПРОИЗВОЛЬНЫХ ТЕПЛОВЫХ УСЛОВИЯХ НА СТЕНКЕ

Аннотация—Наряду с точным определением турбулентных тепловых полей на стенке предлагается новая $\overline{t^2}$–ε_t модель теплопереноса. Предложенная модель адекватно воспроизводит предельные характеристики скорости и температуры при произвольных тепловых условиях на стенке. С целью обобщения применимости $\overline{t^2}$–ε_t модели проведена оценка постоянных и функций модели. Эффективность модели также проверяется при пяти различных типичных распределениях температуры, часто встречающихся в инженерных приложениях, в условиях пристенных турбулентных сдвиговых течений. Результаты расчетов сравниваются с имеющимися экспериментальными данными и результатами моделирования, а также с расчетами по ранее применявшимся моделям. Показано, что предложенная модель намного эффективней предыдущих.